

## Original Article

**Running Title:** *Porphyromonas gingivalis* Infection and HNSCC Development

Received: February 26, 2025; Accepted: October 28, 2025

### Altered *PLAU* Expression in *Porphyromonas gingivalis*-Treated Human Immortalised Oral Epithelial Cells and Its Putative Role in Head and Neck Squamous Cell Carcinoma

Adithyan Kannan<sup>\*,\*\*</sup>, BDS, Vijayashree Priyadharsini Jayaseelan<sup>\*\*♦</sup>, PhD

<sup>\*</sup>Department of Microbiology, Saveetha Dental College and Hospital, Saveetha Institute of Medical and Technical Sciences [SIMATS], Saveetha University, Chennai, India

<sup>\*\*</sup>Clinical Genetics Lab, Centre for Cellular and Molecular Research, Saveetha Dental College and Hospital, Saveetha Institute of Medical and Technical Sciences [SIMATS], Saveetha University, Chennai, India

#### ♦Corresponding Author

Vijayashree Priyadharsini Jayaseelan, PhD

Clinical Genetics Lab,

Centre for Cellular and Molecular Research,

Saveetha Dental College and Hospital,

Saveetha Institute of Medical and Technical Sciences [SIMATS],

Saveetha University, Chennai, India

Email: [vijayashreej.sdc@saveetha.com](mailto:vijayashreej.sdc@saveetha.com)

#### Abstract

**Background:** *Porphyromonas gingivalis*, a key pathogen in periodontitis, has been implicated in oral carcinogenesis. The present study investigated the dysregulated genes in human oral epithelial cells (HOEC) treated with *P. gingivalis* (*Pg*) and explored their potential involvement in the development of head and neck squamous cell carcinoma (HNSCC).

**Method:** A computational design, using GEOmnibus data was employed to extract key information on differentially expressed genes (DEGs) in HOEC treated with *Pg*. A curated list of the top 20 DEGs was then examined for their gene expression profiles and survival rates using the UALCAN database. To explore gene enrichment and protein interaction networks, the Metascape and STRING databases were used. Additionally, the effect of microRNA on the expression profiles of candidate genes shared by both phenotypes was examined using the miRDB portal.

**Results:** Among the 20 genes queried, the *PLAU* gene was found to be upregulated in both the *Pg*-treated cells and the HNSCC dataset. The high expression of this gene correlated with poor prognosis in HNSCC patients. Furthermore, the microRNA *hsa-miR-23b-3p*, identified as targeting *PLAU*, was significantly downregulated, resulting in poor prognosis in HNSCC patients.

**Conclusion:** Our study reveals that *Pg* infection induced significant alterations in the gene expression in HOEC. The *PLAU* gene was identified as an important gene that demonstrated a putative association with periodontal disease and HNSCC. The influence of epigenetic markers, such as non-coding RNAs, and the methylation profile of the gene requires further investigation.

**Keywords:** Bacterial infections, Disease, Genes, Periodontitis, Prognosis

#### Introduction

Head and neck squamous cell carcinoma (HNSCC) arises from the mucosal linings of the oral cavity, larynx and pharynx. The increasing incidence of this cancer type poses a significant global health burden in

developing nations. Smoking, tobacco chewing, alcoholism, poor oral hygiene, sharp tooth, viral infections etc., are considered to be the significant classical risk factors associated with the development of HNSCC. Despite the advancements in the treatment

modality, the survival rate of patients remains very low due to late diagnosis, metastasis, and recurrence. Oral microflora harbors more than 700 species of microorganisms. A balanced microbiome is essential for maintaining both oral and systemic health.<sup>1</sup> Any dysbiosis in the oral microbiome leads to various diseases, including cancer of the oral cavity. Studies have reported alterations in the oral microbiome in oral submucous fibrosis patients, characterized by increased pathogens such as *Fusobacterium*, *Prevotella*, and *Porphyromonas*.<sup>1</sup> Chronic inflammation due to persistent infection acts as a key modifier of the onconiche, potentiating the development or progression of the tumor. A few species of bacteria have been found to produce metabolites and virulence factors that induce genotoxic stress, resulting in DNA damage. The production of reactive oxygen species is one such process that can cause mutations and alterations in the DNA molecule. An impaired DNA repair mechanism invariably contributes to genomic instability.<sup>2</sup>

Among the oral pathogens, *Porphyromonas gingivalis* (*Pg*), a keystone pathogen associated with the development of chronic periodontitis (CP), has been found to play a crucial role in oral carcinogenesis.<sup>3</sup> A systematic review with network analysis conducted by Villar et al. reported a consistent association between periodontal disease and cancers such as oral, lung, pancreatic, gastrointestinal, and colorectal.<sup>4</sup> A study by Woo et al. demonstrated the response of OSCC cells towards chemotherapeutic agents in the presence or absence of *Pg*. A striking presentation of chemoresistance was observed in OSCC cells infected with *Pg*, which was mediated through Notch1 activation.<sup>5</sup> Reports have revealed the molecular mechanisms by which *Pg* regulates the transformation of oral epithelial cells, including modulation of host immune response, triggering cell proliferation, dysregulation of the cell cycle,<sup>6,7</sup> and many more. However, the precise process that leads to dysregulation of the genes upon exposure to the periodontal pathogen is yet to be comprehensively studied.

Recent advancements in high-throughput approaches, such as next-generation sequencing and microarrays, have provided opportunities to dissect the molecular profiles in *Pg*-infected cells. Computational methods have aided in minimizing the time taken for data analysis, curation, and interpretation. Thus, this method has been considered a boon for clinical researchers who intend to identify enigmatic biomarkers related to a specific disease presentation.<sup>8,9</sup> Information on dysregulated genes and altered signaling pathways could offer novel insights into how the pathogen contributes to the development and progression of HNSCC.<sup>10</sup> Identifying these differentially expressed genes (DEGs) is vital not only for understanding the pathophysiology of HNSCC mediated by the exposure of cells to *Pg*, but also for discovering early biomarkers that can serve in early detection of head and neck cancer. Furthermore, the microRNAs targeting the candidate gene and their effect on the prognosis of the HNSCC patient have also been unraveled. DEGs could serve the purpose of therapeutic leads when they are targeted using small molecule inhibitors or non-coding synthetic RNAs.

## Methods

### *Study design*

The present study followed an integrative computational approach that relies on multiple datasets to derive an association between the keystone periodontal pathogen *Porphyromonas gingivalis* (*Pg*) and HNSCC. Several studies have been designed to use the datasets to investigate the disease-pathogen associations earlier.<sup>11,12</sup> Every cell in the human body behaves differently when exposed to a specific stimulus. Thus, it would be more appropriate to study the outcome of pathogen exposure on specific cell types to gain more insights into the molecular basis of disease. Also, identifying key molecular pathways triggered during infection of oral epithelial cells with a single infectious pathogen could provide more information about the pathogen-specific genes and pathways. This is a promising strategy to reveal the possible role of a pathogen in the process of carcinogenesis. This novel

approach may be beneficial to clinical researchers, as it is more cost-effective and less time-consuming.

### **Sample dataset**

The GEOmnibus dataset GSE192887 was used for the study. Immortalized human oral epithelial cells (HOEC) are cells that have been transduced with viral components to prevent senescence and promote proliferation, thereby enabling experimentation in an environment that mimics a human biological system. This series comprised four samples of HOEC infected with *P. gingivalis* (*Pg*) (GSM5767976, GSM5767977, GSM5767978, GSM5767979), three untreated immortalised HOEC (GSM5767973, GSM5767974, GSM5767975). The untreated HOEC cells were taken as the control, and HOEC cells infected with *Pg* were taken as the test group (<https://www.ncbi.nlm.nih.gov/geo/geo2r/?acc=GSE192887>).<sup>13</sup> Benjamini and Hochberg's method was used to derive an adjusted *P*-value, and the *P*-value lower than 0.05 was considered significant. The log 2-fold change threshold was set at 0. Both the parameters log2fold change and adjusted p value were used to perform preliminary curation of the gene list. The pseudogenes and non-coding RNAs were excluded from further analysis.

### **Protein-protein interaction (PPI) analysis**

The analysis focused on the top 20 DEGs to explore their PPIs using the STRING (Search Tool for the Retrieval of Interacting Genes/Proteins) tool, version 12. Various sources were selected for the analysis, including text mining, experiments, databases, co-expression, gene fusion, co-occurrence, and neighborhood. An interaction score of at least 0.400 was established as a criterion. This bioinformatics resource provides insights into direct physical connections and functional relationships between proteins. In the network, proteins are depicted as nodes, while the edges illustrate the type of interactions, including physical, enzymatic, or genetic interactions.<sup>14</sup>

### **Gene ontology analysis**

The PANTHER database (v16.0; Protein Analysis Through Evolutionary Relationships) was employed for gene ontology analysis, which helped us

comprehend the molecular pathways, functions, biological processes, and subcellular locations of gene products. A user-defined query targeting the top 20 genes was executed to ascertain the pathways in which these genes are grouped. Furthermore, pathway-based classification was conducted to investigate potential pathways linked to the genes, enhancing the overall understanding of the analysis.<sup>15,16</sup>

### **Gene enrichment analysis**

Gaining insights from large-scale studies requires pinpointing essential biological pathways and protein complexes in complex datasets. Metascape (v3.5) is an intuitive web portal designed to assist experimental biologists in analyzing and interpreting such data by merging various biological databases and analytical tools. It simplifies the process and provides precise results with features like functional enrichment, interactome analysis, and gene annotation, making it easier for researchers to compare data from different experiments. We used DisGENET analysis to integrate various data types.<sup>17</sup>

### **Gene expression and survival analysis**

The present study examined the top 20 genes exhibiting differential expression in the *Pg*-treated HOEC group through the GEO2R program. This analysis was expanded in the HNSCC dataset available from the UALCAN database (<http://ualcan.path.uab.edu/cgi-bin/TCGA-survival>). It included data from 520 patients with primary HNSCC tumours and 44 corresponding normal samples. Gene expression was quantified in transcripts per million (TPM), which is a standard method for normalizing RNA-seq data. Differences between groups were analyzed using Box-Whisker plots based on the TPM values. Moreover, the study assessed the overall survival rates of HNSCC patients using Kaplan-Meier analysis. By comparing the high-expression and low/medium-expression groups, the present study illustrated the effect of gene expression changes on patients' overall survival.<sup>18</sup> The Kaplan Meier Survival Plotter was further used to confirm the survival status of HNSCC patients upon changes in the gene expression profile of the selected gene [<https://kmplot.com/analysis/>].<sup>19</sup>

### ***Differential Gene Expression Analysis Using TNMplot***

TNMplot (v2) is a web platform that analyses gene expression in tumour, normal, and metastatic tissues (<https://tnmplot.com/analysis/>). It provides valuable insights into the associations between gene expression levels and tumour stages, thereby providing a better understanding of cancer biology. This tool was used to identify the differential gene expression profile of the *PLAU* gene in oral cavity cancer, the predominant form of HNSCC, and others, such as cancers of the nasopharyngeal region and tongue.<sup>20</sup> The non-paired and tumour samples from patients with specific cancer types were compared. The Mann-Whitney test was performed to analyze the significance between the two groups. A *P*-value less than 0.05 was considered to be significant. This data provides supportive evidence on the gene expression pattern of *PLAU* in other types of head and neck cancers.

### ***Statistical analysis***

Gene expression data from various datasets were thoroughly examined with the robust GEO2R tool, which uses R packages from Limma to analyze microarray data and present findings in detailed tables and graphic plots.<sup>21</sup> The UALCAN portal performed an extensive analysis of gene expression profiles by comparing expression levels across groups through a PERL script supported by the Comprehensive Perl Archive Network (CPAN) module. Furthermore, survival plots were created using the "survival" and "survminer" R packages, followed by comparison via the log-rank test. The "survival" package was used for detailed survival analysis, which included survival curves, hypothesis tests, and models. In addition, the "survminer" package notably improved the visualization of Kaplan-Meier and forest plots, promoting clear and comprehensive interpretation of complex survival data.<sup>22</sup>

### ***miRNA expression analysis***

Epigenetic elements, including DNA methylation, histone protein modifications, and non-coding RNAs, play a crucial role in regulating gene expression. Notably,

microRNAs have emerged as significant contributors to cancer phenotypes and are associated with multiple cancer types. Analyzing microRNAs that target the specific gene provides valuable insights into the gene's expression pattern.<sup>23,24</sup> The miRBD database serves as a helpful resource for identifying microRNAs that target specific gene transcripts. When microRNA levels increase, the number of mRNA copies for the targeted gene diminishes which, in turn, leads to decreased protein expression. Consequently, precise prediction of miRNAs targeting DEGs is crucial for comprehending the impact of epigenetic factors in carcinogenesis. This analysis was conducted using the miRDB database (<http://mirdb.org>).

### ***Ethics approval and consent to participate***

The present study followed a computational analysis with datasets available from different sources that are available to the public; therefore, an ethical statement was not required.

## **Results**

### ***Curation of DEGs***

An analysis of the GSE192887 dataset revealed numerous DEGs in HOEC treated with *Pg* (Figure 1). Among the 20 DEGs, twelve were upregulated, and eight were downregulated. The Grainyhead-like transcription factor 3 (*GRHL3*) encoding gene showed the highest level of expression (Log<sub>2</sub> fold = 3.49), and the Plasminogen activator, urokinase (*PLAU*) encoding gene showed the lowest level of expression from the upregulated gene pool (Table 1).

### ***PPI and Gene enrichment analysis***

The PPI network demonstrated that ten protein-encoding genes, *viz.*, *HES1*, *ANGPTL4*, *MYC*, *RHOB*, *PLAU*, *IL1B*, *CXCL1*, *EGR1*, *IRF6*, and *GHRL3*, interact with each other. Two pairs of genes, *S100A2* and *FGFBP1*, *COL7A1* and *PLEC*, exhibit an interaction. Six other genes were found to exist as independent entities (Figure 2). The DisGENET analysis, supported by gene enrichment of the top 20 DEGs curated from the dataset, revealed their enrichment in lip and oral cavity carcinoma and malignant neoplasm of the mouth, head, and neck

carcinoma. The enrichment analysis thus provided preliminary results about the possible association of DEGs with oral cavity cancer. Further analysis employing HNSCC patients and the influence of genes on the survival of patients was investigated (Figure 3).

#### **Gene ontology analysis**

The gene ontology analysis performed using PATHER revealed 19 significant pathways. Notably, the pathway associated with the highest number of genes was the chemokine and cytokine signaling pathway (CCKR), commonly associated with inflammation. One or a few genes were also clustered within the NOTCH, PDGF, Wnt, and p53 signaling pathways related to oral carcinogenesis. This highlights its potential role in the cellular response to *Pg* infection and its involvement in developing HNSCC (Figure 4).

#### **Gene expression and survival analysis**

The expression profile revealed 11 genes to be upregulated, two to be downregulated, and seven with insignificant expression among HNSCC patients (Table 2). The *PLAU* gene was the only gene to exhibit a similar expression pattern in both the *Pg*-treated HOEC and HNSCC datasets. This gene demonstrated a significant difference between the normal and primary tumour tissue. The median TPM value was much higher (171.289) in the primary tumour group when compared with normal (16.267), equating to a *P*-value significance of  $<10^{-12}$ . The survival analysis also revealed a substantial difference between the low/medium and high expression groups, wherein the high expression patients succumbed to poor prognosis ( $P = 0.0025$ ). The KM plotter also confirmed the survival status of HNSCC patients presenting with differential expression of the *PLAU* gene. Here, the high-expression cohort exhibited a low survival rate with a median survival of 35.97 months compared with the low-expression cohort with 68.8 months, with the *P*-value of significance being 0.00027 (Figure 5).

#### **Gene expression in HNSCC types**

An increased expression of *PLAU* was observed in HNSCC patients. The median gene expression value was 667 for normal and 1635 for tumour, with a *P*-value of

0.0209. The oral cavity cancer showed an upregulation of *PLAU* with a median expression value of 424 and 2996 in normal and tumour tissues, respectively, with a *P*-value of  $6.03 \times 10^{-09}$ . The nasopharyngeal and tongue cancer also showed a significant upregulation of *PLAU* with a *P*-value of  $5.02 \times 10^{-07}$  and  $1.2 \times 10^{-06}$  (Figure 6).

#### **miRNA expression analysis**

An investigation of the top 10 non-coding RNAs (Table 3) targeting the *PLAU* gene revealed one microRNA, i.e., *hsa-miR-23b-3p*, to be downregulated ( $5.99 \times 10^{-05}$ ). The expression profile was also found to influence the prognosis of HNSCC patients ( $P = 0.0035$ ), with patients in the low- to medium-expression group presenting a poorer prognosis. The Kaplan-Meier plotter demonstrated that the median survival months for the low-expression cohort were 46.47 months, and for the high-expression cohort, they were 66.73 months, with a *P*-value of 0.00052 (Figure 7).

#### **Discussion**

Periodontitis (PD) is a locally destructive, chronic, inflammatory process that has been related to an increased risk of cancer. A few common factors, such as smoking, alcoholism, and poor oral hygiene, have been found to affect both the phenotypes of cancer and PD. A study by Zhang et al. reported almost twice the number of periodontal cases in 2019 compared with 1990. These numbers are quite bewildering as they can add to the escalating incidence of oral cancer observed in developing countries.<sup>25</sup> Upon investigation of the aetiology of PD, several periodontopathic pathogens, such as *Porphyromonas gingivalis* (*Pg*), *Tannerella forsythia* (*Tf*), *Treponema denticola* (*Td*), *Fusobacterium nucleatum* (*Fn*), *Aggregatibacter actinomycetemcomitans* (*Aa*), and many more pathogens, were found to increase the risk of cancer in various populations. An extensive text-mining approach provided substantial evidence of the association of *Pg* and *Fn* with numerous cancer types, including cancers of the head and neck region.<sup>26,27</sup> With the clue derived from previous studies, we analyzed underlying molecular mechanisms that could

drive the transformation of normal cells exposed to *Pg* infection using a computational approach. We found the *PLAU* gene might be critical in establishing the cancer phenotype in *Pg*-infected oral epithelial cells. The expression pattern was similar in almost all tissues of the head and neck region, including the tongue and nasopharynx. Further, the cognate microRNA, *hsa-miR-23b-3p*, was identified as a vital regulator of *PLAU* gene expression.

Experimental and clinical studies have demonstrated the consequences of *Pg* infection on normal and cancerous cells. Ha et al. investigated the outcomes of *Pg*-infection of oral cancer cells. In addition to morphological changes observed in the cancer cells exposed to *Pg*, an increased expression of CD44 and CD133, unique cancer stem cell markers, was also observed. The invasiveness observed also correlated well with the upregulation of MMP1 and MMP10 induced by IL-8.<sup>28</sup> Geng et al. have shown that persistent exposure of human immortalized oral epithelial cells to *Pg*-induced morphological changes and increased proliferative ability, markedly influencing the cell migratory potential and invasiveness.<sup>7</sup> The elevated protein glycogen synthase kinase-3 beta, an epithelial-mesenchymal transition (EMT) regulator, increased over time. Also, the protein Vimentin significantly increased over the 120<sup>th</sup> hour of *Pg* infection. A decrease in the expression of E-cadherin and beta-catenin, with an increase in MMP protein, was also evidenced.<sup>29</sup>

The *PLAU* gene encodes the plasminogen activator urokinase (uPA), which is often dysregulated in various cancer types. A similar study by Chen et al. revealed that *PLAU* could induce EMT, thereby influencing the prognosis of HNSCC patients. In line with these facts, the present study demonstrated that DEG, *PLAU* is a candidate gene with prognostic significance in HNSCC patients. An extensive analysis using multiple computational tools revealed a strong association of the *PLAU* gene with HNSCC. This result was further confirmed using *in situ*, *in vitro*, and *in vivo* models. The CAL27 cell line, an epithelial cell line derived from the tongue of a male patient diagnosed with

squamous cell carcinoma, was used for this purpose. The transfection of CAL27 with *PLAU*-siRNA suppressed their proliferation and migration. Quantitative real-time PCR analysis showed an increase in the levels of the epithelial-mesenchymal marker, E-cadherin, and decreased levels of N-cadherin, fibronectin, *ZEB1*, *ZEB2*, *SNAIL*, *TWIST1*, and *TWIST2*.<sup>30</sup>

A very recent study by Hamada et al. demonstrated the ability of *Pg* to support the tumour phenotype. Several genes related to the migration of tumour cells were identified. Protein-protein network analysis and Cox regression analysis revealed that high expression of *PLAU* leads to poor prognosis in HNSCC patients.<sup>31</sup> Another study by Lu et al. demonstrated the downregulation of ZFP36 in response to persistent infection with *Pg*. This condition enhanced the tumour-related biological transformation of human-immortalized oral epithelial cells.<sup>32</sup> The *PLAU* gene exhibited a similar prognosis in bladder urothelial carcinoma. The gene expression was significantly higher in bladder urothelial carcinoma patients, which correlated with a poor prognosis in patients receiving Atezolizumab. An increased expression of the *PLAU* gene was related to advanced TNM staging and tumour immune infiltration. The *PLAU* knockdown inhibited proliferative ability, invasiveness, and aggressiveness in bladder cancer phenotypes.<sup>33</sup> The exploration of the functions of *PLAU* gene product on esophageal squamous cell carcinoma (ESCC) revealed that it contributed to the heterogeneity of cancer-associated fibroblasts. The increased protein expression resulted in the activation of the MAPK pathway with a concomitant increase in Slug and MMP9, triggering cancer cell proliferation and clone formation. The U0126, a MEK 1/2 inhibitor, reversed the cancer phenotype thus observed.<sup>34</sup>

Epigenetic and epi-transcriptomic modifications have emerged as novel regulators of carcinogenesis. Common mechanisms such as methylation, histone modifications and regulation of gene expression by non-coding RNAs form the basis of epigenetic regulation.<sup>35-37</sup>

Conversely, the chemical modifications of RNA, such as m6A and 5mC, can modulate their function, stability, localization, and translation.<sup>38</sup> The present study identified a microRNA, *hsa-miR-23b-3p*, among the top 10 microRNAs queried and classified based on their target scores. Accumulating evidence has shown that overexpression of *hsa-miR-23b-3p* suppresses EMT in human cervical cancer CasKi cells.<sup>39</sup> Previous studies have proved the tumour suppressive activity of *hsa-miR-23b-3p* in different cancer types. *hsa-miR-23b-3p* was found to repress the expression of c-Met, thereby altering the CasKi and C33A cell's properties, conferring the ability to divide uncontrollably, migrate, and invade tissues.<sup>40</sup>

Our study investigated the molecular connections between periodontal disease caused by *Pg* and the development of HNSCC. It adds to the current understanding of the involvement of periodontal pathogens in oral cancer. The present study systematically identified genes with altered expression levels and their implications in cancer progression. The analysis was also expanded to identify epigenetic components that can target candidate genes, thereby shedding light on the broader gene regulation network and its impact on cancer outcomes. Our study has also laid the groundwork for exploring targeted therapies that could address the link between chronic oral infections and malignancies of the head and neck region. The upregulation of *PLAU* in both the *Pg*-treated cells and the HNSCC dataset, which has a poor prognosis, unequivocally underscores its potential as a novel biomarker indicating disease progression. These findings suggest that the dysregulation of the *PLAU* gene and the microRNA present a critical link between periodontal infection and HNSCC. However, the influence of other epigenetic factors on this relationship warrants further investigation to understand the multifaceted mechanisms driving this association entirely. The present study provides valuable insights that will undoubtedly pave the way for novel therapeutic approaches targeting gene regulation in the prevention and treatment of

CP in individuals at risk of developing HNSCC.

With all its merits addressed, the study had certain limitations, including (a) the process leading to the immortalization of oral epithelial cells involved in the use of viruses. Although the control group was an untreated cell of the same type, normal oral keratinocytes or fibroblasts could be used to acquire a more intense understanding of the molecular pathways triggered or suppressed during the infection with *Pg*, (b) a small sample group was employed in the PD dataset which could have an influence on the curated list of genes, (c) secondly, the study group employed consisted of a mixed population rather than a specific ethnic group. Thus, the geographical variations should also be considered to confirm disease associations, (d) the demographic details of the HNSCC patients included smoking and alcohol history, but there are several other factors such as tobacco chewing, passive smoking, exposure to chemicals or environmental components that could have influenced the gene expression process, (e) next, while microRNAs were investigated in the present study, there are other epigenetic mechanisms such as DNA methylation and histone modifications which could have a profound impact on the gene expression profile, (f) finally, the comparison of multiple datasets and conducting experiments using in-vitro, in-vivo models could aid in gathering better knowledge about the involvement of genes and pathways triggered during infection with *Pg*. Therefore, analyzing several other components of the carcinogenesis process holds excellent promise for deciphering a more concrete gene-disease association.

## Conclusion

The present integrated computational analysis provides comprehensive and valuable insights into the molecular mechanisms underlying the oral epithelial cell response to *Pg* infection and its potential association with HNSCC. According to the study results, the *PLAU* gene emerged as a significant player among the top 20 DEGs assessed. The upregulation of the *PLAU* gene correlated well with the poor prognosis in HNSCC patients, making it

a candidate gene for theragnostic interventions. The pathway and network analysis lead to several crucial observations about the process of carcinogenesis driven by the *PLAU* gene. The observations on the downregulation of the microRNA, *has-miR-23b*, a potential target of *PLAU* gene transcripts, open new avenues to develop therapeutic modalities based on the epigenetic marks, especially the non-coding RNAs. Furthermore, functional analysis of the upstream and downstream targets of this gene and the gene network could substantiate their role in establishing carcinogenesis in different populations exposed to various etiological factors.

### Acknowledgments

The authors thank the participants in the TCGA cohort study. We also thank the developers of the GEOmnibus and UALCAN databases, without whom clinical researchers would not have been able to perform such an analysis.

### Authors' Contributions

AK: Study design, data accumulation, conducting analysis, original draft preparation; JVP: Conceptualization, result analysis, interpretation, consolidation of results, review of original draft. All authors have read and approved the final manuscript and agreed to be accountable for all aspects of the work in ensuring that questions related to the accuracy or integrity of any part of the work are appropriately investigated and resolved.

### Funding

Not applicable.

### Conflict of Interest

None declared.

### References

1. Aghili S, Rahimi H, Hakim LK, Karami S, Soufdoost RS, Oskouei AB, et al. Interactions between oral microbiota and cancers in the aging community: A narrative review. *Cancer Control*. 2024;31:10732748241270553. doi: 10.1177/10732748241270553. PMID: 39092988; PMCID: PMC11378226.
2. Kashyap B, Kullaa A. Salivary metabolites produced by oral microbes in oral diseases and oral squamous cell carcinoma: A review. *Metabolites*. 2024;14(5):277. doi: 10.3390/metabo14050277. PMID: 38786754; PMCID: PMC11122927.
3. Farhad SZ, Karbalaehasanesfahani A, Dadgar E, Nasiri K, Esfahaniani M, Nabi Afjadi M. The role of periodontitis in cancer development, with a focus on oral cancers. *Mol Biol Rep*. 2024;51(1):814. doi: 10.1007/s11033-024-09737-6. PMID: 39008163.
4. Villar A, Mendes B, Viègas M, de Aquino Alexandre AL, Paladini S, Cossatis J. The relationship between periodontal disease and cancer: Insights from a Systematic Literature Network Analysis. *Cancer Epidemiol*. 2024;91:102595. doi: 10.1016/j.canep.2024.102595. PMID: 38878682.
5. Woo BH, Kim DJ, Choi JI, Kim SJ, Park BS, Song JM, et al. Oral cancer cells sustainedly infected with *Porphyromonas gingivalis* exhibit resistance to Taxol and have higher metastatic potential. *Oncotarget*. 2017;8(29):46981-92. doi: 10.18632/oncotarget.16550. PMID: 28388583; PMCID: PMC5564538.
6. Groeger SE, Hudel M, Zechel-Gran S, Herrmann JM, Chakraborty T, Domann E, et al. Recombinant *Porphyromonas gingivalis* W83 FimA alters immune response and metabolic gene expression in oral squamous carcinoma cells. *Clin Exp Dent Res*. 2022;8(4):976-87. doi: 10.1002/cre2.588. PMID: 35570325; PMCID: PMC9382057.
7. Geng F, Liu J, Guo Y, Li C, Wang H, Wang H, et al. Persistent exposure to *Porphyromonas gingivalis* promotes proliferative and invasion capabilities, and tumorigenic properties of human immortalized oral epithelial cells. *Front Cell Infect Microbiol*. 2017;7:57. doi: 10.3389/fcimb.2017.00057. PMID: 28286742; PMCID: PMC5323389.
8. He B, Cao Y, Zhuang Z, Deng Q, Qiu Y, Pan L, et al. The potential value of oral

- microbial signatures for prediction of oral squamous cell carcinoma based on machine learning algorithms. *Head Neck*. 2024;46(7):1660-70. doi: 10.1002/hed.27795. PMID: 38695435.
9. Belibasakis GN, Seneviratne CJ, Jayasinghe RD, Vo PT, Bostanci N, Choi Y. Bacteriome and mycobiome dysbiosis in oral mucosal dysplasia and oral cancer. *Periodontol 2000*. 2024;96(1):95-111. doi: 10.1111/prd.12558. PMID: 38501658; PMCID: PMC11579824.
  10. Bs A, P A, As SG, A P, J VP. Analysis of differentially expressed genes in dysplastic oral keratinocyte cell line and their role in the development of HNSCC. *J Stomatol Oral Maxillofac Surg*. 2024;125(4S):101928. doi: 10.1016/j.jormas.2024.101928. PMID: 38815724.
  11. M D, P A, Smiline Girija AS, A P, Priyadharsini J V. Differential gene expression profile in *Porphyromonas gingivalis* treated human gingival keratinocytes and their role in the development of HNSCC. *J Oral Biol Craniofac Res*. 2025;15(1):48-56. doi: 10.1016/j.jobcr.2024.11.007. PMID: 39717877; PMCID: PMC11664403.
  12. Shanmugam SB, Vijayashree Priyadharsini J, Anitha P, Smiline Girija AS, Paramasivam A. Dysregulated genes in HIGK-treated *F. nucleatum* and their possible association with HNSCC. *Mol Biol Res Commun*. 2025;14(1):59-71. doi: 10.22099/mbrc.2024.50171.1982. PMID: 39744516; PMCID: PMC11624608.
  13. Liu M, Shao J, Zhao Y, Ma B, Ge S. *Porphyromonas gingivalis* evades immune clearance by regulating lysosome efflux. *J Dent Res*. 2023;102(5):555-64. doi: 10.1177/00220345221146097. PMID: 36800907.
  14. Szklarczyk D, Gable AL, Lyon D, Junge A, Wyder S, Huerta-Cepas J, et al. STRING v11: protein-protein association networks with increased coverage, supporting functional discovery in genome-wide experimental datasets. *Nucleic Acids Res*. 2019;47(D1):D607-D613. doi: 10.1093/nar/gky1131. PMID: 30476243; PMCID: PMC6323986.
  15. Mi H, Thomas P. PANTHER pathway: an ontology-based pathway database coupled with data analysis tools. *Methods Mol Biol*. 2009;563:123-40. doi: 10.1007/978-1-60761-175-2\_7. PMID: 19597783; PMCID: PMC6608593.
  16. Mi H, Ebert D, Muruganujan A, Mills C, Albu LP, Mushayamaha T, et al. PANTHER version 16: a revised family classification, tree-based classification tool, enhancer regions and extensive API. *Nucleic Acids Res*. 2021;49(D1):D394-D403. doi: 10.1093/nar/gkaa1106. PMID: 33290554; PMCID: PMC7778891.
  17. Zhou Y, Zhou B, Pache L, Chang M, Khodabakhshi AH, Tanaseichuk O, et al. Metascape provides a biologist-oriented resource for the analysis of systems-level datasets. *Nat Commun*. 2019;10(1):1523. doi: 10.1038/s41467-019-09234-6. PMID: 30944313; PMCID: PMC6447622.
  18. Chandrashekar DS, Karthikeyan SK, Korla PK, Patel H, Shovon AR, Athar M, et al. UALCAN: An update to the integrated cancer data analysis platform. *Neoplasia*. 2022;25:18-27. doi: 10.1016/j.neo.2022.01.001. PMID: 35078134; PMCID: PMC8788199.
  19. Györfy B. Integrated analysis of public datasets for the discovery and validation of survival-associated genes in solid tumors. *Innovation (Camb)*. 2024;5(3):100625. doi: 10.1016/j.xinn.2024.100625. PMID: 38706955; PMCID: PMC11066458.
  20. Bartha Á, Györfy B. TNMplot.com: A Web Tool for the Comparison of Gene Expression in Normal, Tumor and Metastatic Tissues. *Int J Mol Sci*. 2021;22(5):2622. doi: 10.3390/ijms22052622. PMID: 33807717; PMCID: PMC7961455.
  21. Barrett T, Wilhite SE, Ledoux P, Evangelista C, Kim IF, Tomashevsky M, et al. NCBI GEO: archive for functional genomics data sets-update. *Nucleic Acids Res*. 2013;41(Database issue):D991-5. doi: 10.1093/nar/gks1193. PMID: 23193258; PMCID: PMC3531084.
  22. Chandrashekar DS, Bashel B, Balasubramanya SAH, Creighton CJ, Ponce-Rodriguez I, Chakravarthi BVSK,

- et al. UALCAN: A portal for facilitating tumor subgroup gene expression and survival analyses. *Neoplasia*. 2017;19(8):649-58. doi: 10.1016/j.neo.2017.05.002. PMID: 28732212; PMCID: PMC5516091.
23. Chen Y, Wang X. miRDB: an online database for prediction of functional microRNA targets. *Nucleic Acids Res*. 2020;48(D1):D127-D131. doi: 10.1093/nar/gkz757. PMID: 31504780; PMCID: PMC6943051.
24. Liu W, Wang X. Prediction of functional microRNA targets by integrative modeling of microRNA binding and target expression data. *Genome Biol*. 2019;20(1):18. doi: 10.1186/s13059-019-1629-z. PMID: 30670076; PMCID: PMC6341724.
25. Zhang X, Wang X, Wu J, Wang M, Hu B, Qu H, et al. The global burden of periodontal diseases in 204 countries and territories from 1990 to 2019. *Oral Dis*. 2024;30(2):754-68. doi: 10.1111/odi.14436. PMID: 36367304.
26. Yuan Q, Wu H, Tan H, Wang X, Cao Y, Chen G. Oral microbial dysbiosis driven by periodontitis facilitates oral squamous cell carcinoma progression. *Cancers (Basel)*. 2025;17(13):2181. doi: 10.3390/cancers17132181. PMID: 40647479; PMCID: PMC12249316.
27. Yáñez L, Soto C, Tapia H, Pacheco M, Tapia J, Osses G, et al. Co-culture of *P. gingivalis* and *F. nucleatum* synergistically elevates IL-6 expression via TLR4 signaling in oral keratinocytes. *Int J Mol Sci*. 2024;25(7):3611. doi: 10.3390/ijms25073611. PMID: 38612423; PMCID: PMC11011619.
28. Ha NH, Woo BH, Kim DJ, Ha ES, Choi JI, Kim SJ, et al. Prolonged and repetitive exposure to *Porphyromonas gingivalis* increases aggressiveness of oral cancer cells by promoting acquisition of cancer stem cell properties. *Tumour Biol*. 2015;36(12):9947-60. doi: 10.1007/s13277-015-3764-9. PMID: 26178482.
29. Lee J, Roberts JS, Atanasova KR, Chowdhury N, Han K, Yilmaz Ö. Human primary epithelial cells acquire an epithelial-mesenchymal-transition phenotype during long-term infection by the oral opportunistic pathogen, *Porphyromonas gingivalis*. *Front Cell Infect Microbiol*. 2017;7:493. doi: 10.3389/fcimb.2017.00493. PMID: 29250491; PMCID: PMC5717492.
30. Chen G, Sun J, Xie M, Yu S, Tang Q, Chen L. PLAU promotes cell proliferation and epithelial-mesenchymal transition in head and neck squamous cell carcinoma. *Front Genet*. 2021;12:651882. doi: 10.3389/fgene.2021.651882. PMID: 34093649; PMCID: PMC8173099.
31. Hamada M, Inaba H, Nishiyama K, Yoshida S, Yura Y, Matsumoto-Nakano M, et al. Transcriptomic analysis of *Porphyromonas gingivalis*-infected head and neck cancer cells: Identification of PLAU as a candidate prognostic biomarker. *J Cell Mol Med*. 2024;28(4):1-18. doi: 10.1111/jcmm.18167. PMID: 38363001; PMCID: PMC10870695.
32. Lu Z, Cao R, Geng F, Pan Y. Persistent infection with *Porphyromonas gingivalis* increases the tumorigenic potential of human immortalised oral epithelial cells through ZFP36 inhibition. *Cell Prolif*. 2024;57(6):e13609. doi: 10.1111/cpr.13609. PMID: 38351596; PMCID: PMC11150143.
33. Shi K, Zhou J, Li M, Yan W, Zhang J, Zhang X, et al. Pan-cancer analysis of PLAU indicates its potential prognostic value and correlation with neutrophil infiltration in BLCA. *Biochim Biophys Acta Mol Basis Dis*. 2024;1870(2):166965. doi: 10.1016/j.bbdis.2023.166965. PMID: 38000776.
34. Fang L, Che Y, Zhang C, Huang J, Lei Y, Lu Z, et al. PLAU directs conversion of fibroblasts to inflammatory cancer-associated fibroblasts, promoting esophageal squamous cell carcinoma progression via uPAR/Akt/NF-κB/IL8 pathway. *Cell Death Discov*. 2021;7(1):32. doi: 10.1038/s41420-021-00410-6. PMID: 33574243; PMCID: PMC7878926.
35. K P A, Usman P P AS, Sekar D. OIP5-AS1 expression profiles in different stages

- of oral squamous cell carcinoma. *Arch Oral Biol.* 2025;180:106403. doi: 10.1016/j.archoralbio.2025.106403. PMID: 41014896.
36. Thomas P, Selvakumar SC, Preethi KA, Sekar D. Expression profiling of signal transducer and activator of transcription3 in oral squamous cell carcinoma in south Indian population. *Minerva Dent Oral Sci.* 2024;73(1):37-44. doi: 10.23736/S2724-6329.23.04840-4. PMID: 37878241.
37. Neralla M, S H, Selvakumar SC, Preethi KA, Sekar D. Gene expression analysis of microRNA-1285 in the South Indian oral squamous cell carcinoma population. *Minerva Dent Oral Sci.* 2024;73(5):249-55. doi: 10.23736/S2724-6329.23.04798-8. PMID: 37410075.
38. Muthumanickam P, Ramasubramanian A, Pandi C, Kannan B, Pandi A, Ramani P, et al. The novel m6A writer methyltransferase 5 is a promising prognostic biomarker and associated with immune cell infiltration in oral squamous cell carcinoma. *J Oral Pathol Med.* 2024;53(8):521-9. doi: 10.1111/jop.13568. PMID: 38939970.
39. Hu J, Sun Z, Hu K, Tang M, Sun S, Fang Y, et al. Over-expression of Hsa-miR-23b-3p suppresses proliferation, migration, invasion and epithelial-mesenchymal transition of human cervical cancer CasKi cells. *Xi Bao Yu Fen Zi Mian Yi Xue Za Zhi.* 2020;36(11):983-9. Chinese. PMID: 33210592.
40. Campos-Viguri GE, Peralta-Zaragoza O, Jiménez-Wences H, Longinos-González AE, Castañón-Sánchez CA, Ramírez-Carrillo M, et al. MiR-23b-3p reduces the proliferation, migration and invasion of cervical cancer cell lines via the reduction of c-Met expression. *Sci Rep.* 2020;10(1):3256. doi: 10.1038/s41598-020-60143-x. PMID: 32094378; PMCID: PMC7039958.

Table 1. List of top 20 differentially expressed genes in *Porphyromonas gingivalis*-treated HOEC compared to untreated HOEC cells

Gene	Protein encoded	Adjusted <i>P</i> value	Log2 fold change	Gene expression
<i>IL1B</i>	Interleukin 1 beta	$1.99 \times 10^{-254}$	1.59	Upregulated
<i>RHOB</i>	Ras homolog family member B	$5.89 \times 10^{-254}$	-1.69	Downregulated
<i>IRF6</i>	Interferon regulatory factor 6	$6.23 \times 10^{-225}$	1.46	Upregulated
<i>CYP24A1</i>	Cytochrome P450 family 24 subfamily A member 1	$6.17 \times 10^{-151}$	1.77	Upregulated
<i>C1orf74</i>	Chromosome 1 open reading frame 74	$2.74 \times 10^{-145}$	1.98	Upregulated
<i>S100A2</i>	S100 calcium binding protein A2	$1.3 \times 10^{-138}$	-1.65	Downregulated
<i>HES2</i>	Hes family bHLH transcription factor 2	$8.83 \times 10^{-134}$	1.89	Upregulated
<i>ANGPTL4</i>	Angiopoietin like 4	$1.79 \times 10^{-95}$	-1.55	Downregulated
<i>CXCL1</i>	C-X-C motif chemokine ligand 1	$6.22 \times 10^{-84}$	1.38	Upregulated
<i>PLAU</i>	Plasminogen activator, urokinase	$7.6 \times 10^{-83}$	0.88	Upregulated
<i>COL7A1</i>	Collagen type VII alpha 1 chain	$1.82 \times 10^{-82}$	-0.93	Downregulated
<i>FAM110C</i>	Family with sequence similarity 110 member C	$1.09 \times 10^{-81}$	-1.05	Downregulated
<i>GRHL3</i>	Grainyhead like transcription factor 3	$2.09 \times 10^{-81}$	3.49	Upregulated
<i>VGLL3</i>	Vestigial like family member 3	$4.67 \times 10^{-79}$	1.17	Upregulated
<i>HES1</i>	Hes family bHLH transcription factor 1	$1.02 \times 10^{-75}$	1.43	Upregulated
<i>FGFBP1</i>	Fibroblast growth factor binding protein 1	$1.07 \times 10^{-75}$	1.16	Upregulated
<i>PLEC</i>	Plectin	$3.25 \times 10^{-75}$	-0.82	Downregulated
<i>G0S2</i>	G0/G1 switch 2	$1.62 \times 10^{-74}$	-0.98	Downregulated
<i>MYC</i>	MYC proto-oncogene, bHLH transcription factor	$4.25 \times 10^{-74}$	0.89	Upregulated
<i>EGR1</i>	Early growth response 1	$2.93 \times 10^{-73}$	-1.05	Downregulated

An adjusted P-value less than 0.05 was considered to be significant; HOEC: Human oral epithelial cells

Table 2. The comparison of gene expression profiles in PG-treated HOEC and HNSCC patients.

Gene	Gene expression in PG treated HOEC	Gene expression in HNSCC	P-value	Survival (P-value)	Survival outcome
<i>IL1B</i>	Upregulated	Upregulated	$1.11 \times 10^{-16}$	0.68	Insignificant
<i>RHOB</i>	Downregulated	Upregulated	$7.19 \times 10^{-03}$	0.36	Insignificant
<i>IRF6</i>	Upregulated	Upregulated	$2.98 \times 10^{-12}$	0.22	Insignificant
<i>CYP24A1</i>	Upregulated	Upregulated	$3.66 \times 10^{-05}$	0.32	Insignificant
<i>C1orf74</i>	Upregulated	Upregulated	$1.88 \times 10^{-15}$	0.45	Insignificant
<i>S100A2</i>	Downregulated	Upregulated	$1.82 \times 10^{-09}$	0.93	Insignificant
<i>HES2</i>	Upregulated	Upregulated	$<10^{-12}$	1.00	Insignificant
<i>ANGPTL4</i>	Downregulated	Upregulated	$2.72 \times 10^{-02}$	0.66	Insignificant
<i>CXCL1</i>	Upregulated	Insignificant	$1.61 \times 10^{-01}$	$<0.00$	High expression, poor prognosis
<b><i>PLAU*</i></b>	<b>Upregulated</b>	<b>Upregulated</b>	<b><math>&lt;10^{-12}</math></b>	<b><math>&lt;0.00</math></b>	<b>High expression, poor prognosis</b>
<i>COL7A1</i>	Downregulated	Upregulated	$1.62 \times 10^{-12}$	0.42	Insignificant
<i>FAM110C</i>	Downregulated	Insignificant	$5.45 \times 10^{-01}$	0.22	Insignificant
<i>GRHL3</i>	Upregulated	Downregulated	$4.35 \times 10^{-05}$	0.08	Insignificant
<i>VGLL3</i>	Upregulated	Insignificant	$9.00 \times 10^{-02}$	0.14	Insignificant
<i>HES1</i>	Upregulated	Insignificant	$9.14 \times 10^{-02}$	0.56	Insignificant
<i>FGFBP1</i>	Upregulated	Insignificant	$8.07 \times 10^{-01}$	0.50	Insignificant
<i>PLEC</i>	Downregulated	Upregulated	$<10^{-12}$	0.50	Insignificant
<i>GOS2</i>	Downregulated	Insignificant	$8.04 \times 10^{-01}$	0.47	Insignificant
<i>MYC</i>	Upregulated	Insignificant	$2.88 \times 10^{-01}$	0.81	Insignificant
<i>EGR1</i>	Downregulated	Downregulated	$8.28 \times 10^{-05}$	0.81	Insignificant

A P-value less than 0.05 was considered to be significant; HOEC: Human oral epithelial cells; HNSCC: Head and neck squamous cell carcinoma; *PLAU\**: Only gene among the top 20 genes curated for analysis demonstrating similar expression in both groups correlating with poor prognosis

Table 3. List of microRNAs targeting the *PLAU* gene, their expression, and survival analysis in HNSCC patients

Target rank	microRNA	miRNA expression in HNSCC cases	<i>P</i> -value	Survival ( <i>P</i> -value)	Survival outcome
1	<i>hsa-miR-6131</i>	Insufficient data			
2	<i>hsa-miR-5692a</i>	Insufficient data			
3	<i>hsa-miR-193b-3p</i>	Upregulated	$1.62 \times 10^{-12}$	0.82	Insignificant
4	<i>hsa-miR-3606-5p</i>	Insufficient data			
5	<i>hsa-miR-193a-3p</i>	Upregulated	$5.08 \times 10^{-07}$	0.99	Insignificant
6	<i>hsa-miR-8485</i>	Insufficient data			
7	<i>hsa-miR-4262</i>	Insufficient data			
8	<i>hsa-miR-3190-5p</i>	Insignificant	$7.98 \times 10^{-01}$	0.86	Insignificant
9	<i>hsa-miR-23a-3p</i>	Upregulated	$2.37 \times 10^{-08}$	0.78	Insignificant
<b>10</b>	<b><i>hsa-miR-23b-3p*</i></b>	<b>Downregulated</b>	<b><math>5.99 \times 10^{-05}</math></b>	<b>0.0035</b>	<b>Poor prognosis</b>

A *P*-value less than 0.05 was considered to be significant; HNSCC: Head and Neck Squamous Cell Carcinoma. *hsa-miR-23b-3p\** is the only target microRNA among the top 10 microRNAs demonstrating a significant downregulation in expression, correlating with poor prognosis.

**Volcano plot**  
**GSE192887: 9 human epithelial cell**  
**transcriptome sequencing analysis**  
**HOEC-PG treated vs HOEC-untreated,  $P_{adj} < 0.05$**

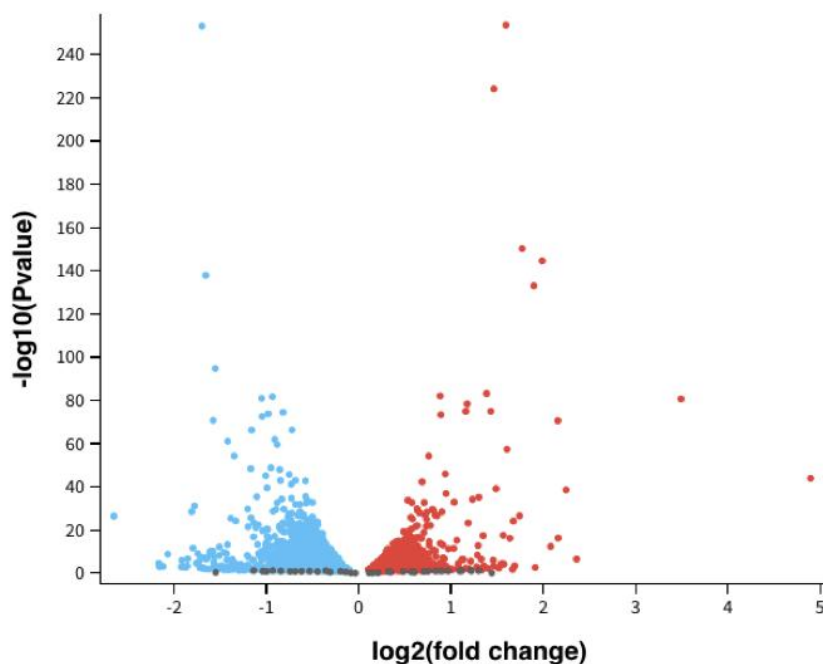


Figure 1. Volcano plot demonstrating the differentially expressed genes induced by *Porphyromonas gingivalis* infection of HOEC. The x-axis shows the log<sub>2</sub> fold change in gene expression in HOEC treated with *Pg* compared with untreated HOEC, with positive values indicating upregulation and negative values indicating downregulation. The y-axis shows the -log<sub>10</sub> of the *P*-value, representing the statistical significance of the observed changes. Red dots indicate genes with significant upregulation ( $P_{adj} < 0.05$ ), while blue dots represent genes with significant downregulation.

An adjusted *P*-value less than 0.05 was considered to be significant; HOEC: Human oral epithelial cells.

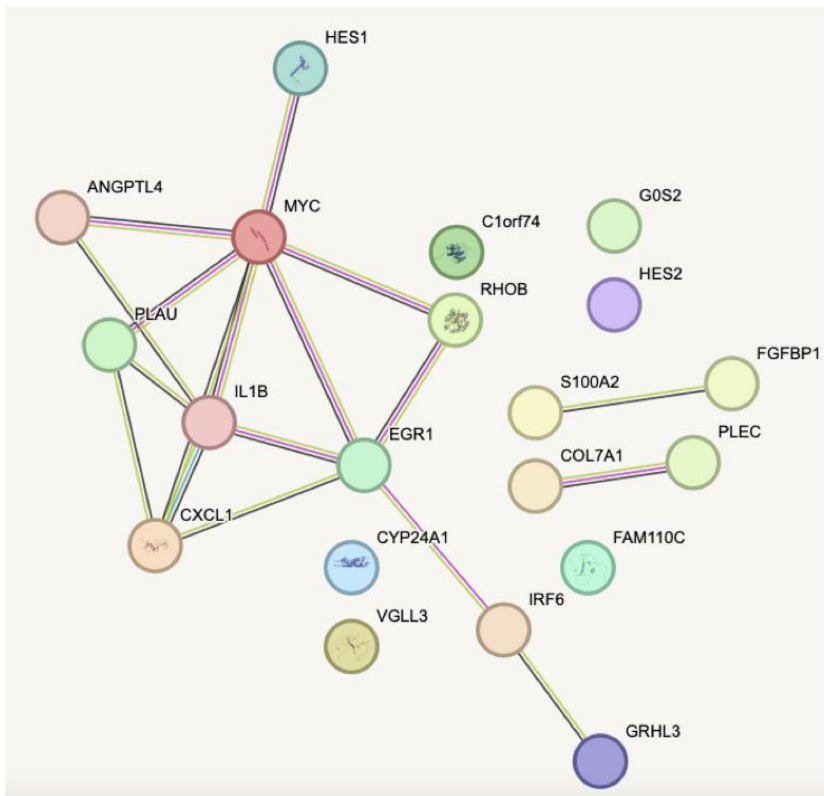


Figure 2. Protein-protein interaction network of the top 20 differentially expressed genes in *Porphyromonas gingivalis*-treated HOEC. There were 20 nodes with 18 edges. The PPI enrichment value was found to be  $2.49 \times 10^{-05}$ .

HOEC: Human oral epithelial cells; PPI: Protein-Protein Interaction

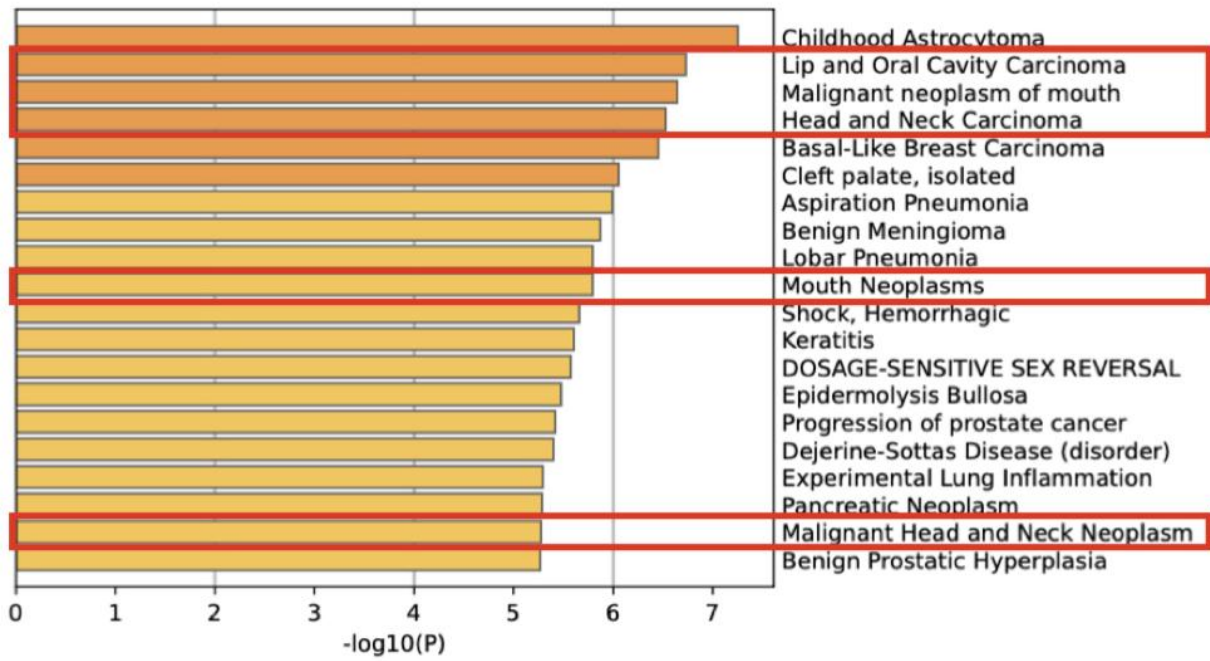


Figure 3. DisGeNET revealed that the pathways encompassing DEGs were associated with lip and oral cavity carcinoma, malignant mouth neoplasms, head and neck carcinoma, mouth neoplasms, and malignant head and neck neoplasms.

DEGs: Differentially expressed genes

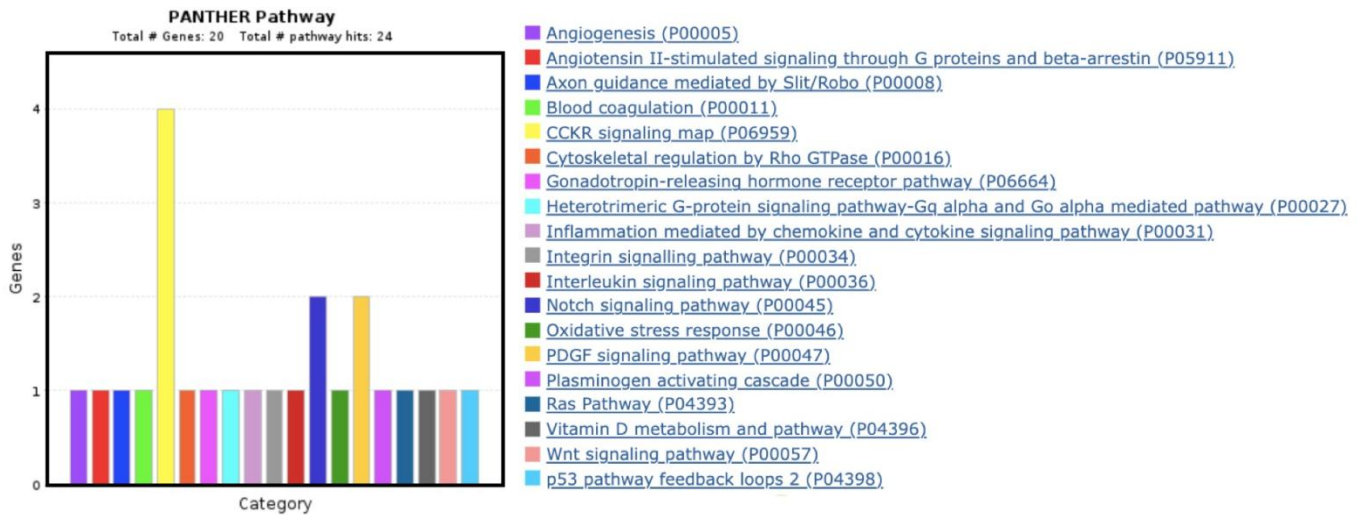


Figure 4. The PANTHER pathway analysis of dysregulated genes in human oral epithelial cells treated with *Porphyromonas gingivalis*. The x-axis represents various biological pathways, and the y-axis shows the number of dysregulated genes associated with each pathway. Each colored bar corresponds to a specific pathway, as the color-coded legend on the right.

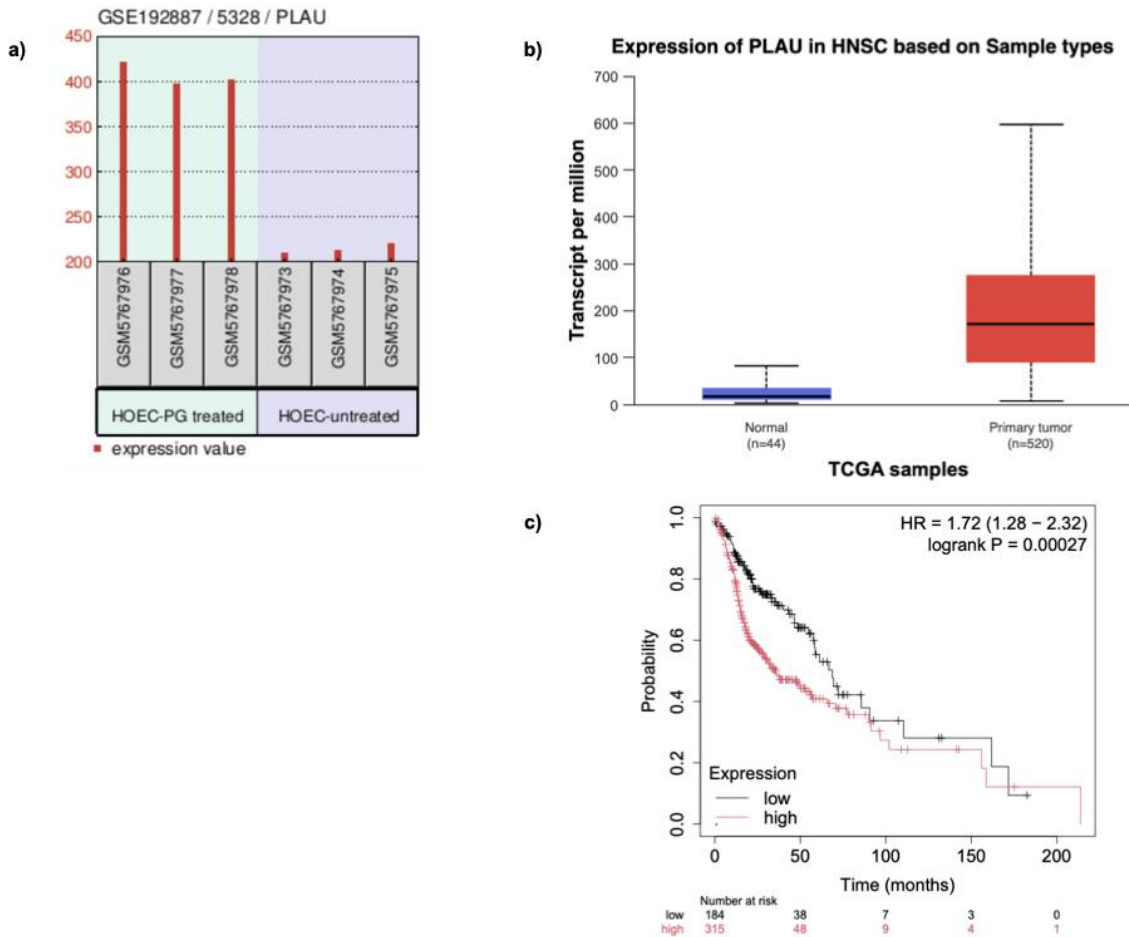
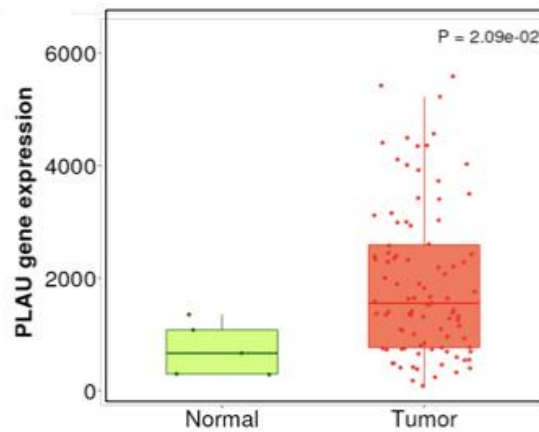


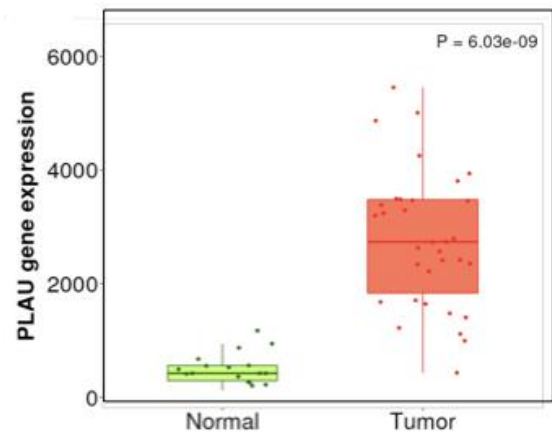
Figure 5. (a) Bar graph representing the differential expression of the *PLAU* gene in human oral epithelial cells treated with *Porphyromonas gingivalis*, (b) Box Whisker plot demonstrating the upregulation of *PLAU* gene in primary tissues of HNSCC patients ( $P$ -value =  $<10^{-12}$ ), (c) Kaplan Meier Plotter demonstrated that patients presenting with high expression of *PLAU* gene exhibited a poor survival rate ( $P = 0.00027$ ).

A  $P$ -value less than 0.05 was considered to be significant.

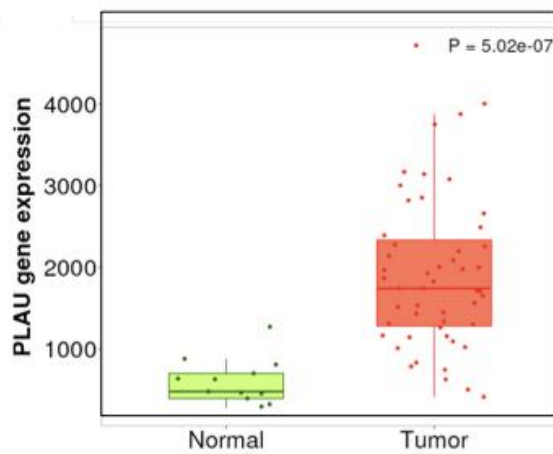
**(a) Head and neck cancer**



**(b) Cancer of oral cavity**



**(c) Cancer of the nasopharyngeal region**



**(d) Cancer of the tongue**

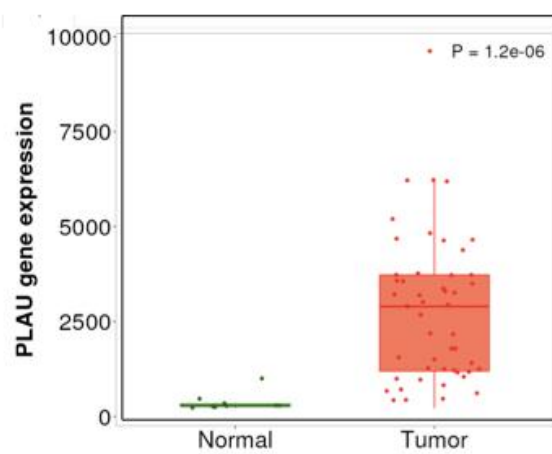


Figure 6. Box Whisker plot demonstrating the *PLAU* gene expression profile in (a) head and neck cancer ( $P$ -value =  $2.09 \times 10^{-2}$ ), (b) cancer of oral cavity ( $P$ -value =  $6.03 \times 10^{-9}$ ), (c) cancer of the nasopharyngeal region ( $P = 5.02 \times 10^{-7}$ ), (d) cancer of the tongue ( $P = 1.2 \times 10^{-6}$ ). A  $P$ -value less than 0.05 was considered to be significant.

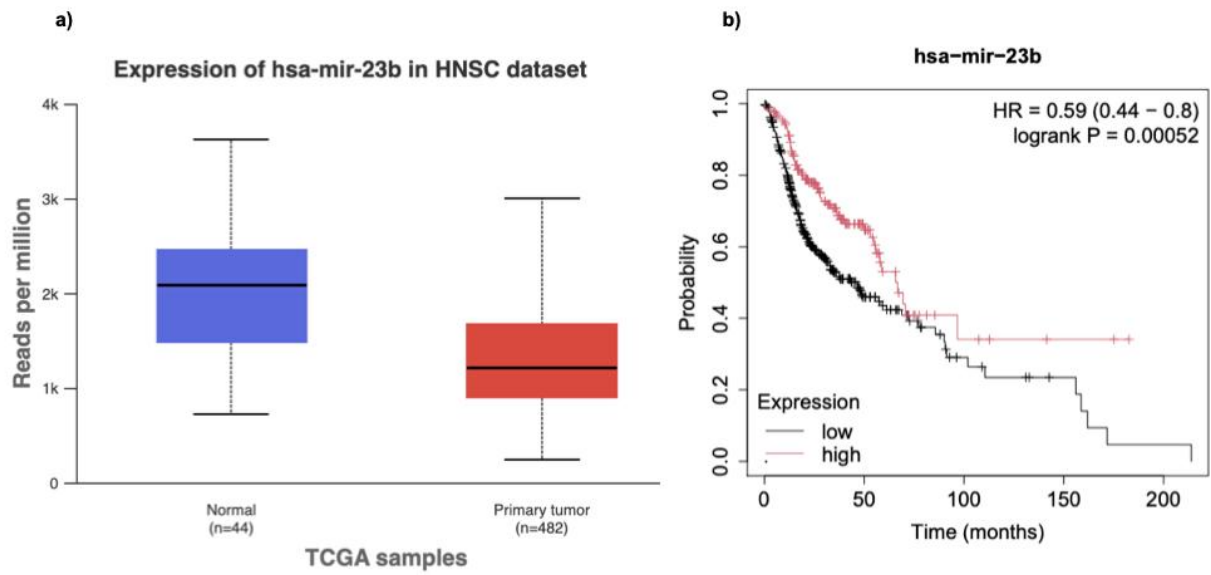


Figure 7. (a) Box Whisker plot demonstrating the downregulation of *hsa-miR-23b-3p* miRNA in primary tissues of HNSCC patients ( $P$ -value =  $5.99 \times 10^{-05}$ ), (b) Kaplan Meier Plotter demonstrated that patients presenting with low/medium expression of *hsa-miR-23b-3p* exhibited a poor survival rate ( $P$ -value = 0.00052).

A  $P$ -value less than 0.05 was considered to be significant.